




Plasticity in dormancy behaviour of *Calanoides acutus* in Antarctic coastal waters

Tristan E. G. Biggs ^{1,2*}, Corina P. D. Brussaard^{1,2}, Claire Evans³, Hugh J. Venables⁴, and David W. Pond⁵

¹Department of Marine Microbiology and Biogeochemistry, NIOZ Royal Netherlands Institute for Sea Research, University of Utrecht, Texel, The Netherlands

²Department of Freshwater and Marine Ecology, Institute for Biodiversity and Ecosystem Dynamics (IBED), University of Amsterdam, Amsterdam, The Netherlands

³Ocean Biogeochemistry & Ecosystems Research Group, National Oceanography Centre, Southampton, UK

⁴British Antarctic Survey, Natural Environmental Research Council, Cambridge, UK

⁵Institute of Aquaculture, University of Stirling, Stirling, Scotland, UK

*Corresponding author: tel: +44 (0) 7977113863; e-mail: tristan.biggs@nioz.nl.

Biggs, T. E. G., Brussaard, C. P. D., Evans, C., Venables, H. J., and Pond, D. W. Plasticity in dormancy behaviour of *Calanoides acutus* in Antarctic coastal waters. – ICES Journal of Marine Science, doi:10.1093/icesjms/fsaa042.

Received 28 October 2019; revised 10 February 2020; accepted 15 February 2020.

Copepods that enter dormancy, such as *Calanoides acutus*, are key primary consumers in Southern Ocean food webs where they convert a portion of the seasonal phytoplankton biomass into a longer-term energetic and physiological resource as wax ester (WE) reserves. We studied the seasonal abundance and lipid profiles of pre-adult and adult *C. acutus* in relation to phytoplankton dynamics on the Western Antarctic Peninsula. Initiation of dormancy occurred when WE unsaturation was relatively high, and chlorophyll *a* (Chl *a*) concentrations, predominantly attributable to diatoms, were reducing. Declines in WE unsaturation during the winter may act as a dormancy timing mechanism with increased Chl *a* concentrations likely to promote sedimentation that results in a teleconnection between the surface and deep water inducing ascent. A late summer diatom bloom was linked to early dormancy termination of females and a second spawning event. The frequency and duration of high biomass phytoplankton blooms may have consequences for the lifespan of the iteroparous *C. acutus* females (either 1 or 2 years) if limited by a total of two main spawning events. Late summer recruits, generated by a second spawning event, likely benefitted from lower predation and high phytoplankton food availability. The flexibility of copepods to modulate their life-cycle strategy in response to bottom-up and top-down conditions enables individuals to optimize their probability of reproductive success in the very variable environment prevalent in the Southern Ocean.

Keywords: copepod, dormancy, life cycle, lipids, phytoplankton, wax ester unsaturation

Introduction

Lipid-rich copepods are important conduits of carbon flow from the base of the marine food web to higher trophic levels and support fish, mammal and seabird communities (Pervushin, 1968; Hopkins and Torres, 1989; Voronina, 1998). At high latitudes, primary production is strongly influenced by the availability of light resulting in distinct phytoplankton bloom cycles and a

relatively short productive season (Ma *et al.*, 2014). As the photoperiod increases after the winter minimum, the annual onset of stratification initiates the highly productive phytoplankton “Spring” bloom (Sverdrup, 1953; Huisman *et al.*, 1999). The life cycles of copepods are strongly affected by this distinct seasonality, and they have developed specific adaptations to take advantage of short-term food availability to survive long periods of

food scarcity. Calanoid copepods are an ecologically important order of marine copepods and several species, particularly those in the Calanidae and Eucalanidae families (Baumgartner and Tarrant, 2017), undergo ontogenetic vertical migration from relatively shallow to deep water where they spend a large proportion of their life cycle in dormancy (Hagen et al. 1993; Sartoris et al., 2010), a resting stage with reduced metabolism and swimming activity (Maps et al., 2014). To outlast the winter months, these copepods accumulate large lipid stores within a membrane-bound oil sac that can occupy a large part of the body cavity (Lee et al., 2006). Not only does this lipid store have to provide fuel for metabolic processes during dormancy, but also it must provide the energy needed to re-ascend to the surface, continue development to adulthood, and fuel early egg production (Pond et al., 2012). As in other oceans, copepods dominate the mesozooplankton across most of the Southern Ocean, in terms of biomass, abundance, grazing activity, and secondary production (Atkinson et al., 2012b). *Calanoides acutus* is a major contributor to zooplankton biomass (Shreeve et al., 2005; Marrari et al., 2011) and an abundant species of herbivorous copepod that spends a large proportion of their life cycle (up to 7–9 months) in dormancy (Hagen et al., 1993; Drits et al., 1994; Tarling et al., 2004; Atkinson et al., 2012b). Mating occurs in deep water during late winter and the males perish shortly after while the females migrate to surface waters to feed on the phytoplankton bloom and begin spawning at the start of spring/summer. Nauplii and early copepodites develop in the euphotic zone until vertical migration to deeper water of pre-adult (CIV and CV) and adult (CVI) stages at the end of summer when feeding in surface waters is terminated (Atkinson et al., 1997; Tarling et al., 2004). Little is known about the life span of overwintered late stage copepodites with some studies suggesting a 1 year life cycle (Marin, 1988; Atkinson et al., 1997) whilst others suggest that individuals may re-enter dormancy and survive an extra year (Drits et al., 1994; Hagen and Schnack-Schiel, 1996).

Prior to dormancy, overwintering stages concentrate phytoplankton lipids and accumulate large stores of total lipid (TL), mainly as wax esters (WEs). High concentrations of TL can be accumulated per individual (>500 µg) representing an energy-rich food source for higher trophic levels (such as fish) and a large reservoir of essential fatty acids (FAs) such as 20:5(n-3) (eicosapentaenoic acid, EPA) and 22:6(n-3) (docosahexaenoic acid). This accumulation of lipids represents the long-term storage of short-term phytoplankton production. The presence or absence of copepod species that enter dormancy plays a fundamental role on a global scale in determining whether or not a region supports a lipid-rich food web (Record et al., 2018). The timing and duration of dormancy has implications for carbon flow as ontogenetic vertical migration events (VMEs) dictate time periods when stored lipids (carbon) are either available in surface waters or sequestered to the deep ocean due to respiration during dormancy (Jónasdóttir et al., 2015). Potential triggers influencing vertical distribution patterns have been identified, such as lipid accumulation above a threshold level (Rey-Rassat et al., 2002; Maps et al., 2012) and utilization during dormancy (Johnson et al., 2008); however, cues remain poorly understood and seasonal datasets are scarce. Following the development of a population over an entire life cycle could provide a better understanding of how these mechanisms influence behaviour. Pond et al. (2012) showed that a critical minimum threshold of ~50% WE unsaturation within the copepod is important for dormancy initiation. The

composition of these lipids, and not the bulk amount, then provides the ability of the WE store to shift from a liquid to a solid phase allowing dormant copepods to become neutrally buoyant in cold deep water and conserve energy (Visser and Jónasdóttir, 1999; Lee et al., 2006; Pond and Tarling, 2011). Although copepod species that enter a period of dormancy have evolved in the open ocean, where such a strategy could provide a key evolutive advantage, genetic programming of individuals that inhabit relatively shallow coastal and shelf sea environments is likely to result in the accumulation of large WE reserves with high levels of unsaturation (Falk-Petersen et al., 2009; Clark et al., 2012). As the FA component of WE is mainly derived from the diet, a suitable food source is critical. High proportions of FA 16:1(n-7), 20:5(n-3), 18:4(n-3), and 22:6(n-3) in storage lipids indicate the importance of diatoms and dinoflagellates in the zooplankton diet (Graeve et al., 1994; Falk-Petersen et al., 2000; Budge et al., 2006). Diatoms often dominate the biomass of phytoplankton blooms in the Southern Ocean (Ducklow et al., 2012) and are an important source of primary nutrition as they produce long-chain polyunsaturated FAs (PUFAs) [such as 20:5(n-3)] in abundance (Kattner and Hagen, 2009). The timing and duration of blooms varies spatially and temporally, as a result of physicochemical factors, and could help explain why the timing of descent in dormancy inducing copepods can be so variable between regions and years (Heath et al., 2004; Johnson et al., 2008; Pepin and Head, 2009). More research is required to better understand the trophic transfer of lipids, particularly in a time of global climate change shown to affect the composition, timing, and magnitude of phytoplankton blooms (Smetacek and Nicol, 2005; Sommer and Lengfellner, 2008; Rozema et al., 2017). These changes are expected to have major implications for the capacity of copepods to undertake their seasonal life cycles successfully (Pond et al., 2014). Understanding population dynamics is fundamental to predict how copepods might respond to future climate change and how Antarctic ecosystems may be influenced by bottom-up forcing.

In this study, in Ryder Bay on the Western Antarctic Peninsula, the lipid content and composition of *C. acutus* individuals (the pre-adult CV and adult CVI) were analysed over a “summer (S1)–winter–summer (S2)” time series and the FA composition was determined to investigate links between the accumulation and composition of WE and diet. Research in the Southern Ocean often focuses on copepods inhabiting the deep-water open ocean (>500–1000 m depth); however, many populations successfully overwinter in relatively shallow coastal and shelf sea environments (<500 m depth, Clark et al., 2012). Ryder Bay is a marginal habitat that is relatively advection free due to localized gyre-like circulation features (Beardsley et al., 2004; Moffat et al., 2008; personal observation), which promotes the retention of phytoplankton and zooplankton populations. This study, which repeatedly sampled the same population in the same local area, is one of very few that presents complete seasonal sampling, including winter and the transition periods between winter and the productive summer, and provides valuable information to better understand the behaviour of copepods in a coastal environment.

Methods

Sample collection

This study was conducted at the Rothera time series site (RaTS, latitude 67.572°S; longitude 68.231°W, bottom depth 520 m) in Ryder Bay on the Western Antarctic Peninsula (Figure 1).

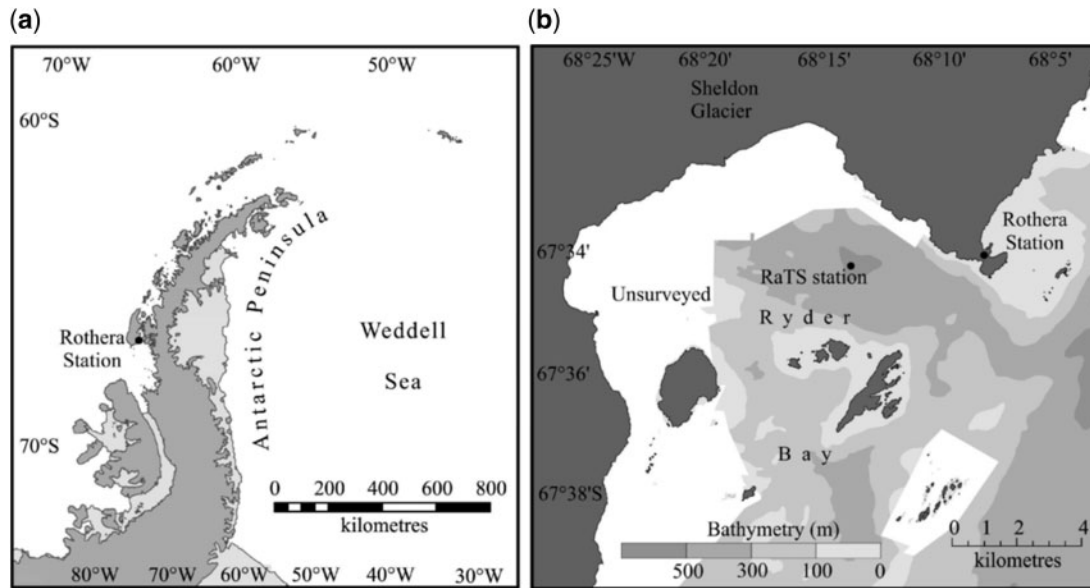


Figure 1. Map of the sampling area: (a) location of Rothera station on the northern tip of Marguerite Bay along the Western Antarctic Peninsula and (b) large-scale map of the sampling site (RaTS) within Ryder Bay and close to Rothera station.

Seawater samples for chlorophyll *a* (Chl *a*) concentration and taxonomic composition analysis were collected from the standard monitoring depth of 15 m by using a 12-l Niskin bottle deployed from a small boat. One to eight litres were filtered over GF/F glass fibre filters (47 mm, Whatman, Eindhoven, The Netherlands), after which the filters were carefully folded and wrapped in aluminium foil, snap-frozen in liquid nitrogen, and stored at -80°C until analysis in the home laboratory using high-performance liquid chromatography (HPLC) and chemical taxonomy analysis [CHEMTAX, see Biggs *et al.* (2019) for methodological details].

Calanoides acutus samples were collected from two depth profiles, i.e. 500–200 m (deep) and 200–0 m (shallow), to separate the overwintering “winter” population from the active “summer” population (Huntley and Escritor, 1991; Schnack-Schiel *et al.*, 1991). A 200- μm mesh ring net (0.26 m² opening) was used to obtain population abundance counts (copepodite stages CI–CVI) in shallow water, and a 500- μm mesh ring net (0.26 m² opening equipped with a double release mechanism) was used to obtain CV (pre-adult) and CVI (adult males and females) individuals from both shallow and deep water. Sampling of copepods occurred weekly (weather dependent) during summer 1 (S1, 23 November 2012–18 April 2013) and summer 2 (S2, 14 November 2013–21 February 2014). To include community dynamics year round, sampling was performed on three occasions during “winter”. Zooplankton were kept in a plastic portable cooler and transported back to the laboratory within 2 h of capture. *Calanoides acutus* in good condition were quickly sorted for lipid analysis using a binocular microscope and the remainder (of the net haul) preserved in 200 ml of formaldehyde (5% final concentration), and stored at 4°C . Formaldehyde-preserved zooplankton samples were split (1/3) using a plankton splitter, and abundances were determined under a binocular microscope.

Lipid analysis

A total of 331 samples of *C. acutus* were collected for lipid analysis consisting of 1635 individuals. Lipids were extracted from

stage CV and CVI (male and female) following Pond and Tarling (2011). Individuals and bulk samples were initially transferred to 1.1-ml tapered vials (Chromacol) containing 500 μl of chloroform:methanol (2:1 v:v) and stored at -80°C . After transport to the home laboratory, the solvent containing each *C. acutus* sample was pipetted into 8-ml glass vials using glass pipettes. The 1.1-ml vials (containing the exoskeleton) were briefly re-extracted and vortexed a further three times with 1 ml chloroform:methanol (2:1 v:v), and the final volume was adjusted to 4 ml. After the addition of 1 ml of potassium chloride (0.88% w:v), samples were vortexed and centrifuged for 2 min at $400 \times g$ to promote phase separation. The lower chloroform phase, containing the TL extract, was removed using Hamilton glass syringes containing a Teflon tipped plunger, into pre-weighed 4-ml glass vials before being evaporated under nitrogen and stored in a vacuum desiccator overnight prior to reweighing.

Lipid class analysis

Aliquots of TL (10 μg) were subjected to high-performance thin-layer chromatography (HPTLC) using a hexane:4 diethyl ether:acetic acid (90:10:1) solvent system (Pond and Tarling, 2011). The plates were sprayed with 8% (v:v) phosphoric acid containing 3% (w:v) copper acetate solution, followed by heating at 160°C for 13 min to char the lipid classes and create dark areas on the HPTLC plate. Lipid classes were then quantified by scanning densitometry (Shimadzu Dual-wavelength TLC Scanner, CS-930), the different lipid classes being identified by comparison with known standards (Pond *et al.*, 1995). The degree of WE unsaturation was used to calculate an unsaturation index as described in Pond and Tarling (2011). In short, HPTLC separated the WEs into two bands: the upper band was rich in saturated fatty and monounsaturated FAs and the lower band was dominated by PUFAs. The unsaturation index was calculated by dividing the amount of PUFA WE by the total WE, providing an index of the degree of unsaturation ranging between 0 and 1.0 (Stevens *et al.*, 2004) and presented as a percentage between 0 and 100%.

FA analysis of TL

Dried aliquots of 150 μg of TL were used for FA analysis. Samples were derivatized with 1 ml of 2% sulphuric acid–methanol (after the addition of standards: 5 μg 19:0 and 1 μg 12:0) and incubated for 4 h at 80°C. After cooling in water, 2 ml of Milli-Q water and 2 ml of hexane were added and vortexed and the upper layer was transferred to a 10-ml glass vial. Two millilitres of hexane was added once more and vortexed, and the upper layer was transferred to a 10-ml glass vial. The sample containing the FA methyl esters was transferred in 200 μl of hexane to a 2-ml vial and stored at -20°C until analysis on a ULTRA Trace gas chromatograph (GC). The GC was equipped with a BPX-70 column with hydrogen as the carrier gas.

Statistics

Comparisons of FA and WE unsaturation data were performed by linear regression in SigmaPlot V14.0 (Systat Software Inc., San Jose, CA, USA).

Results

Two main periods of phytoplankton accumulation occurred in S1 (2012–2013), 30 November–2 January and 11 February–15 April (Figure 2), as indicated by Chl *a* dynamics, which were dominated by diatoms ($86 \pm 14\%$ $n=13$ and $88 \pm 19\%$ $n=17$, of total Chl *a*, respectively; Biggs et al., 2019). Female *C. acutus* are important for population growth (due to spawning) and contributed most across all time points to populations in both shallow ($37 \pm 40\%$, $n=32$) and deep ($61 \pm 33\%$, $n=28$) water. At the start of S1, females were the most abundant stage and only found in deep water (Figure 3a and b) until the abundance of females inhabiting shallow waters (shallow female) increased between 30 November and 12 December (Figure 3b), from 4 to 108 ind 100 m^{-3} , indicating the first ontogenetic VME (VME 1) of S1 and post-winter dormancy termination. The increase in shallow female abundance coincided with a decline in numbers of females inhabiting deep waters (deep females, from 44 to 4 ind 100 m^{-3}) at the same time as rapidly increasing Chl *a* concentrations (from 0.5 to 3.5 $\mu\text{g l}^{-1}$, Figure 2). Following the decline in the initial phytoplankton bloom at the beginning of January in S1 (Figure 2), shallow female numbers began to decline at the same time as a rise in the number of deep females (0–18 ind 100 m^{-3} , Figure 3a) and deep CVs (0–9 ind 100 m^{-3} , Figure 3c), indicating VME 2 (29 December to 17 January) and the descent of individuals to deep water (dormancy initiation). The number of deep females continued to increase until a steep decline between 20 February and 2 March (from 30 to 8 ind 100 m^{-3} , Figure 3a) alongside a brief increase in shallow female abundance (from 8 to 33 ind 100 m^{-3} , Figure 3b) and indicated a third VME (VME 3) and the second ascent of females in S1 (dormancy termination). Chl *a* concentrations had been increasing for 2 weeks prior to VME 3 (from 0.81 to 5.79 $\mu\text{g l}^{-1}$) and a high biomass phytoplankton bloom (max = 16 $\mu\text{g Chl a l}^{-1}$) developed over a period of 2 months (Figure 2).

Copepodite stage CV was, overall, the second most dominant life-cycle stage contributing on average $22 \pm 27\%$ $n=28$ to total numbers. At the beginning of S1, CVs were absent from net hauls (Figure 3c and d) and numbers remained relatively low until a rapid increase in the abundance of CVs inhabiting shallow waters (shallow CVs) between 1 and 20 February (from 12 to 123 ind 100 m^{-3} , Figure 2d), 7–10 weeks after the peak in abundance of

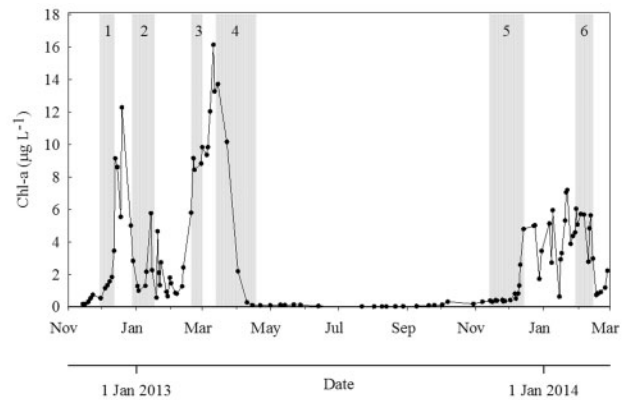


Figure 2. Time series of Chl *a* (as measured by HPLC) at 15-m depth at the sampling site in Ryder Bay. Dashed lines separate time periods of: S1 from 23 November 2012 to 18 April 2013; winter (W) from 19 April 2013 to 13 November 2013 and S2 from 14 November 2013 to 21 February 2014. Shaded areas (grey) represent time periods of VMEs 1–6 as indicated by numbers (1–6) at the top of the chart.

shallow females during VME 1. Numbers of shallow CVs remained high until 13 March (Figure 3d) and declined at the same time as increasing numbers of CVs found in deep water (deep CVs, from 7 to 129 ind 100 m^{-3} , Figure 3c) indicating a fourth VME (VME 4, 13 March to 18 April) and the start of the CV overwintering period (dormancy initiation). Chl *a* concentrations during this late-season diatom bloom peaked on 12 March and declined thereafter, until low concentrations on 15 April (Figure 2) indicated the end of the phytoplankton productive season.

At the beginning of the winter dormancy period (18 April), CVs contributed 88% to total population abundance (Figure 4). A steady decline in the number of deep CVs was observed until 14 November (down to 0 ind 100 m^{-3} , Figure 3c), at the same time as a steady rise in the number of deep females (up to 39 ind 100 m^{-3} , Figure 3a), and indicates the maturation of copepodites from CV to CVI stages. The greatest change in the ratio of CV:CVI occurred between 16 May and 12 August (from 13 to 1) with relatively more males in deep nets on 12 August (30%) than females (18%, Figure 4). Male abundance remained high (and only observed in deep water) until 14 November and declined thereafter to zero by mid-December in S2 (Figure 3e). A 68% decline in population abundance over winter indicates that (in retrospect) each female at VME 1 needed to contribute a minimum of 3 (CV) individuals to the population at the start of the overwintering period (VME 4) to maintain population numbers (at VME 5 compared with VME 1) and offset losses during winter. This suggests that, generally, even low numbers of females can reconstitute the numbers required to ensure the population long-term viability.

At the beginning of S2 (2013–2014), phytoplankton biomass began to slowly increase during November and rapidly increased from 0.4 to 4.8 $\mu\text{g l}^{-1}$ between 2 and 14 December (Figure 2). One extended period of increased Chl *a* concentrations followed (2 December–14 February) with the phytoplankton community continually dominated by diatoms ($83 \pm 15\%$, of Chl *a*, $n=32$; Biggs et al., 2019]. Between 14 November and 14 December, a sharp decline in deep females (39–2 ind 100 m^{-3} , Figure 3a) and

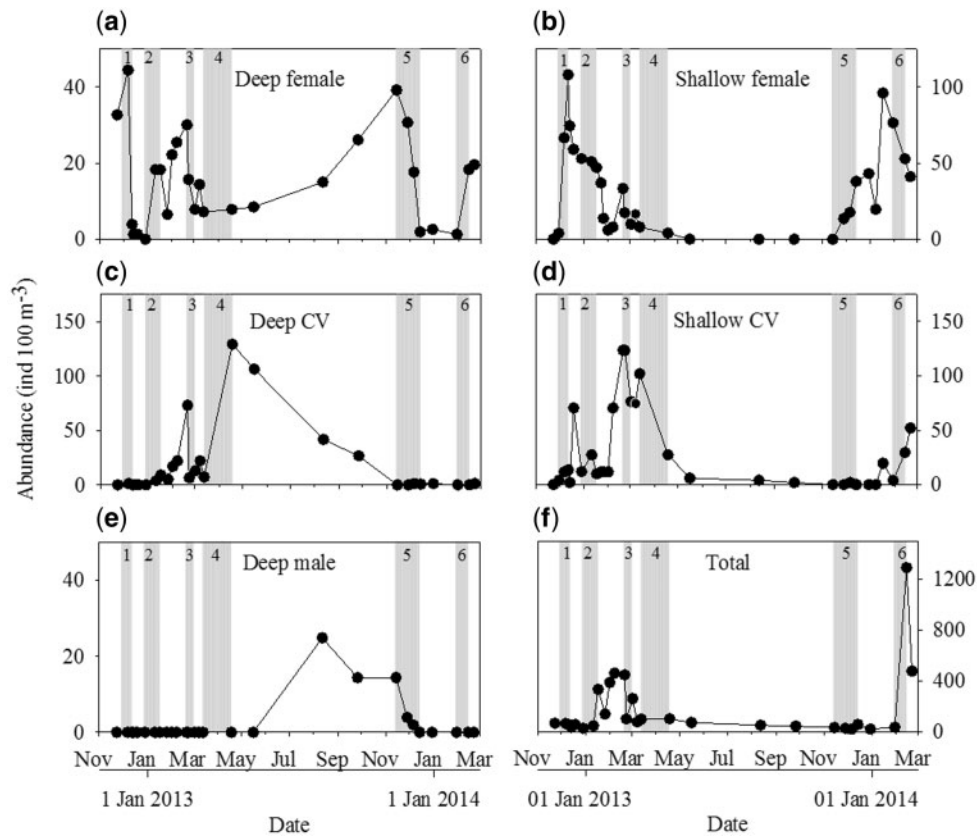


Figure 3. Temporal dynamics of *C. acutus* abundance (ind 100 m⁻³). Deep refers to individuals collected between 500 and 200 m depth and shallow between 200 and 0 m. Shaded areas (grey) represent time periods of VMEs 1–6. (a) The abundance of deep females, (b) the abundance of shallow females, (c) the abundance of deep CVs, (d) the abundance of shallow CVs, (e) the abundance of deep males, and (f) total population abundance (stages CI–CVI). Different y-axis scales between subplots.

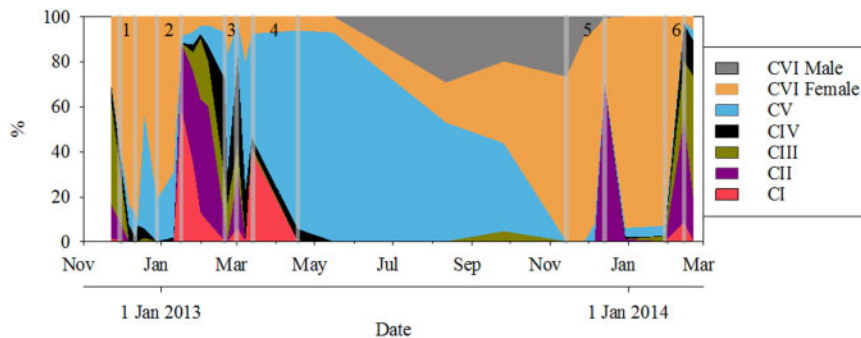


Figure 4. Relative abundance of stage separated *C. acutus* (CI–CVI), with shallow and deep individuals combined, over the study period at the sampling site in Ryder Bay. Grey lines represent time periods (beginning and end) of VMEs 1–6, indicated at the top of the chart.

an increase in shallow females (0–38 ind 100 m⁻³, Figure 3b) indicated a fifth VME (VME 5) and post-winter dormancy termination. Shallow female abundance peaked on 17 January (96 ind 100 m⁻³, Figure 3b) and declined until the end of S2 (41 ind 100 m⁻³); however, the number of deep females remained low until an increase between 30 January and 14 February (from 1 to 18 ind 100 m⁻³, Figure 3a) at the same time as declining surface Chl *a* concentrations (from 5.6 to 0.7 µg l⁻¹ between 12 and 17 February, Figure 2). This indicates a sixth VME (VME 6, 30 January–14 February) and the descent of females at the end of S2

(dormancy initiation). CVs were absent during S2 until an increase in shallow CVs on 17 January (20 ind 100 m⁻³; Figure 3d) that continued until the end of the season (52 ind 100 m⁻³ by 21 February).

When examining the population dynamics of all *C. acutus* copepodite stages (CI–CVI), a period of increased abundance occurred in S1 between 17 January and 2 March 2013 (304 ± 144 ind 100 m⁻³, n = 7, Figure 3f). At the initial increase on 17 January (333 ind 100 m⁻³), a rapid rise in the share of CIs was observed (59%, Figure 4) occurring 5 weeks after the peak in

shallow females at the beginning of S1 (Figure 3b). A second rapid increase in the share of CIs occurred on 13 March (40% of total, Figure 4) when total abundance was lower (97 ind 100 m^{-3}) and 3 weeks after the second peak in numbers of shallow females (33 ind 100 m^{-3} , Figure 3) on 20 February. This indicates two rounds of spawning occurred during S1. During S2, population abundance remained low until a sharp increase on 14 February 2014 (1291 ind 100 m^{-3} , Figure 3f). Only one sharp rise in CI abundance was captured in the dataset during S2 (Figure 4) with 3106 CI–CIV 100 m^{-3} on 14 February in S2 (data not shown) appearing 1 month later than the initial CI increase in S1.

Lipids, WE, and FAs

WEs are often the main type of storage lipid in dormancy inducing copepods and generally dominate TL profiles. In this study, the percentage of TL contained as WEs was $\sim 80\%$ in both females and CVs confirming that WE were the main storage lipid of *C. acutus* individuals (Supplementary Online Resource 1). The TL FA profiles of females were dominated by 20:1(n-9) (18%), 20:5(n-3) (16%), 20:3(n-3) (11%), 16:1(n-7) (11%), and 22:1(n-11) (9%) (Table 1) with CV FA dominated by 20:5(n-3) (21%), 20:1(n-9) (19%), 20:3(n-3) (12%), 22:6(n-3) (9%), and 22:1(n-11) (8%) (Table 2). Male FA profiles were mainly composed of 20:1(n-9) (22%), 22:6(n-3) (19%), 20:5(n-3) (14%), 22:1(n-11) (11%), 10:0 (9%), and 16:0 (8%) (Table 3). FAs were grouped into PUFAs and saturated and monounsaturated FAs (SMUFA) to investigate seasonal unsaturation dynamics in FA data. Of total PUFA, 20:5(n-3) and 20:3(n-3) accounted for the largest share (42 and 26%, respectively) whilst 20:1(n-9), 22:1(n-11), and 16:1(n-7) accounted for the majority of SMUFA (33, 15, and 16%, respectively). When the FA data are combined for CV and CVI stages, linear regressions indicated the concentration of 20:5(n-3) ($\mu\text{g ind}^{-1}$) significantly related to total PUFA ($p < 0.0001$, $r^2 = 0.99$, $n = 18$, Figure 5a) as did % 20:5(n-3) to % of polyunsaturated WEs (PUWEs, $p < 0.0001$, $r^2 = 0.84$, $n = 18$, Figure 5b). Although concentrations of 22:6(n-3) and 20:3(n-3) significantly related to total PUFA ($p < 0.0001$, $r^2 = 0.88$ and 0.77 , respectively, $n = 18$, Figure 5c and e), no significant relationship was observed between % PUWE and both % 22:6(n-3) ($p = 0.061$, $r^2 = 0.20$, $n = 18$, Figure 5d) and % 20:3(n-3) ($p = 0.63$, $r^2 = 0.01$, $n = 18$, Figure 5f). Of the dominant SMUFA, the sum of 20:1(n-9) and 22:1(n-11) FA strongly related to concentrations of total SMUFA ($\mu\text{g ind}^{-1}$, $p < 0.0001$, $r^2 = 0.91$, $n = 18$, Figure 5g) and negatively related to % PUWE ($p < 0.0001$, $r^2 = 0.61$, $n = 18$; Figure 5h). When both % 20:1(n-9) and % 22:1(n-11) were compared with PUWE, both had a significant negative linear relationship ($p = 0.0002$, $r^2 = 0.60$ and $p = 0.0032$, $r^2 = 0.43$, $n = 18$); however, no significant relationship was observed between % 16:1(n-7) and % PUWE ($p = 0.83$, $r^2 = 0.003$, $n = 18$). The FA dataset indicates that the unsaturation dynamics of WE are primarily determined by the accumulation of 20:5(n-3) during the summer and selective utilization of 20:5(n-3) combined with the retention of both 20:1(n-9) and 22:1(n-11) FA during winter.

The TL content of females at the beginning of S1 (23 November) was $112\ \mu\text{g ind}^{-1}$ (Figure 6a) and 28% unsaturation of WE (Figure 7a). TL content and WE unsaturation separated by depth and stage are available in Supplementary Online Resources 2 and 3. During dormancy termination (VME 1, 30 November–

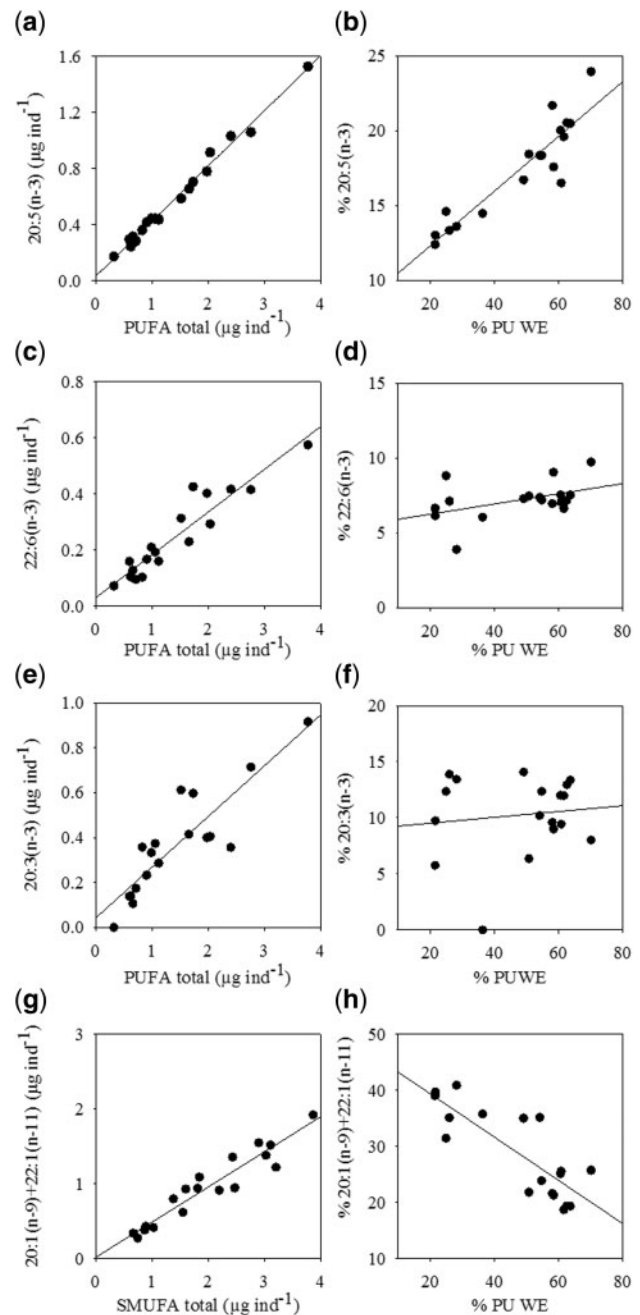


Figure 5. Linear regressions of copepod FAs and % polyunsaturation of total WE (% PUWE) for (a) concentrations of 20:5(n-3) FA vs. PUFA total, (b) % 20:5(n-3) vs. % PUWE, (c) concentrations of 22:6(n-3) FA vs. PUFA total, (d) % 22:6(n-3) vs. % PUWE, (e) concentrations of 20:3(n-3) FA vs. PUFA total, (f) % 20:3(n-3) vs. % PUWE, (g) concentrations of 20:1(n-9) + 22:1(n-11) vs. SMUFAs total, and (h) % 20:1(n-9) + 22:1(n-11) vs. % PUWE. y -Axis scales differ between plots.

12 December), female TL increased slightly to $136.8\ \mu\text{g ind}^{-1}$ and remained relatively constant throughout (131.5 – $141.4\ \mu\text{g ind}^{-1}$, Figure 6a); however, WE unsaturation declined from 31 to 22% (Figure 7a). During VME 2 (dormancy initiation), female TL increased from 124 to $350\ \mu\text{g ind}^{-1}$ (Figure 6a) and WE unsaturation increased from 33 to 49% (Figure 7a). At the beginning of

Table 1. Temporal dynamics of adult female *C. acutus* FAs (FA %) per copepod

CVI female FA %: mean (n = 29)																			
Month year	December 2012		January 2013	February 2013	March 2013		April 2013	May 2013	August 2013	September 2013	November 2013		December 2013		January 2014		February 2014		
Day/FA	19	29	17	20	8	13	18	16	12	26	14	28	6	14	30	17	30	14	21
10:0	6.7	6.4	4.4	4.0	3.0	2.4	0.8	3.1	4.8	3.1	–	5.1	5.9	7.0	9.1	4.9	3.0	3.4	3.3
14:0	5.6	8.2	3.7	4.2	4.0	3.6	4.7	4.2	4.5	4.0	–	5.6	5.1	5.5	6.1	3.8	3.5	3.3	3.7
15:0	0.0	0.0	2.6	2.2	2.8	3.2	0.0	2.3	0.0	0.0	–	0.0	0.0	0.0	0.0	2.5	2.7	3.2	2.0
16:0	4.8	13.1	4.9	4.8	4.3	4.1	9.9	4.5	3.7	4.5	–	6.1	5.7	5.4	6.2	4.7	4.0	3.7	4.5
16:1(n-7)	8.1	5.7	12.5	13.1	11.4	12.4	9.7	12.4	10.3	8.5	–	9.7	8.2	8.7	10.7	10.5	8.6	8.6	9.9
16:4(n-1)	0.0	1.7	5.1	3.7	3.5	3.6	1.0	2.0	0.0	0.0	–	0.0	0.0	0.0	0.0	5.1	4.9	5.5	4.8
17:0	0.0	0.0	2.8	1.5	2.5	3.5	0.0	2.9	0.0	0.0	–	0.0	0.0	0.0	0.0	2.4	2.7	2.8	2.1
18:1(n-9)	3.9	4.3	4.4	4.5	4.3	4.3	4.6	4.8	4.3	4.8	–	4.1	4.5	4.9	4.0	3.4	3.9	4.0	4.8
18:1(n-7)	0.2	0.0	0.0	2.2	1.0	1.9	2.7	2.4	0.0	1.9	–	2.2	1.0	0.0	0.0	0.0	0.0	0.0	0.0
18:4(n-3)	0.0	1.4	4.3	3.6	3.4	4.0	3.5	3.7	0.0	2.0	–	0.0	0.0	0.0	0.0	3.8	3.7	3.3	3.6
20:1(n-9)	30.2	17.2	14.9	15.5	16.9	14.1	12.3	16.0	26.4	23.8	–	21.1	24.9	26.5	26.4	12.5	13.1	13.2	15.2
20:3(n-3)	13.2	0.0	6.4	9.0	11.7	12.2	3.8	11.4	13.7	11.1	–	12.3	13.9	9.7	5.8	12.0	13.4	12.9	9.6
20:4(n-3)	0.0	2.8	1.3	1.0	1.9	2.0	0.0	2.0	2.0	2.4	–	0.0	0.0	0.0	0.0	2.0	2.2	2.2	1.5
22:1(n-11)	10.1	18.6	6.9	7.3	7.7	6.3	15.9	6.9	11.4	10.5	–	10.4	10.2	13.1	12.7	6.2	6.2	6.1	6.5
20:5(n-3)	13.4	14.5	18.4	16.1	15.6	15.5	22.6	14.2	13.6	16.8	–	14.6	13.3	13.0	12.4	19.6	20.5	20.5	21.7
22:6(n-3)	3.8	6.0	7.4	7.4	6.1	6.9	8.5	7.1	5.3	6.6	–	8.8	7.1	6.1	6.6	6.6	7.5	7.2	6.9
Saturated	17.1	27.7	18.4	16.7	16.6	16.9	15.4	17.1	13.1	11.5	–	16.8	16.8	17.9	21.4	18.3	16.0	16.3	15.6
Monounsaturated	52.5	45.8	38.7	42.7	41.3	38.9	45.2	42.5	52.4	49.6	–	47.5	48.9	53.3	53.8	32.7	31.9	32.0	36.3
Polyunsaturated	30.5	26.5	42.8	40.6	42.1	44.2	39.4	40.4	34.6	38.9	–	35.8	34.3	28.9	24.8	49.0	52.2	51.7	48.1

Table 2. Temporal dynamics of pre-adult stage CV *C. acutus* FAs (FA %) per copepod

CV FA %: mean (n = 53)																			
Month year	December 2012		January 2013	February 2013	March 2013		April 2013	May 2013	August 2013	September 2013	November 2013		December 2013		January 2014		February 2014		
Day/FA	19	29	17	20	8	13	18	16	12	26	14	28	6	14	30	17	30	14	21
10:0	–	–	–	1.0	2.4	2.2	2.5	2.8	3.8	4.1	–	–	–	–	–	–	–	–	–
14:0	–	–	–	3.6	2.7	2.8	2.1	2.8	3.6	3.6	–	–	–	–	–	–	–	–	–
15:0	–	–	–	3.1	1.6	0.0	1.7	0.0	0.0	0.0	–	–	–	–	–	–	–	–	–
16:0	–	–	–	5.8	4.1	4.0	4.3	6.4	6.3	4.7	–	–	–	–	–	–	–	–	–
16:1(n-7)	–	–	–	8.2	5.5	5.7	3.6	4.1	5.4	4.8	–	–	–	–	–	–	–	–	–
16:4(n-1)	–	–	–	4.2	5.1	5.0	5.4	5.9	2.2	0.0	–	–	–	–	–	–	–	–	–
17:0	–	–	–	3.0	2.8	0.0	2.8	0.0	0.0	2.7	–	–	–	–	–	–	–	–	–
18:1(n-9)	–	–	–	4.3	3.4	4.0	4.4	3.5	4.3	4.3	–	–	–	–	–	–	–	–	–
18:1(n-7)	–	–	–	3.0	1.0	1.0	0.7	0.0	0.0	0.0	–	–	–	–	–	–	–	–	–
18:4(n-3)	–	–	–	4.0	3.7	3.7	3.8	3.7	2.8	0.0	–	–	–	–	–	–	–	–	–
20:1(n-9)	–	–	–	13.4	15.8	19.2	17.7	27.3	21.7	25.0	–	–	–	–	–	–	–	–	–
20:3(n-3)	–	–	–	9.0	13.0	11.9	9.5	2.7	7.4	16.0	–	–	–	–	–	–	–	–	–
20:4(n-3)	–	–	–	1.3	2.1	1.3	0.0	2.4	0.0	0.0	–	–	–	–	–	–	–	–	–
22:1(n-11)	–	–	–	6.3	7.3	8.6	7.2	7.5	11.4	10.4	–	–	–	–	–	–	–	–	–
20:5(n-3)	–	–	–	19.1	21.2	22.6	24.4	24.2	22.2	16.6	–	–	–	–	–	–	–	–	–
22:6(n-3)	–	–	–	10.7	8.3	7.9	10.2	6.8	9.0	7.7	–	–	–	–	–	–	–	–	–
Saturated	–	–	–	16.5	13.5	9.1	13.3	12.0	13.7	15.2	–	–	–	–	–	–	–	–	–
Monounsaturated	–	–	–	35.2	33.1	38.6	33.5	42.3	42.7	44.5	–	–	–	–	–	–	–	–	–
Polyunsaturated	–	–	–	48.3	53.4	52.3	53.3	45.7	43.6	40.3	–	–	–	–	–	–	–	–	–

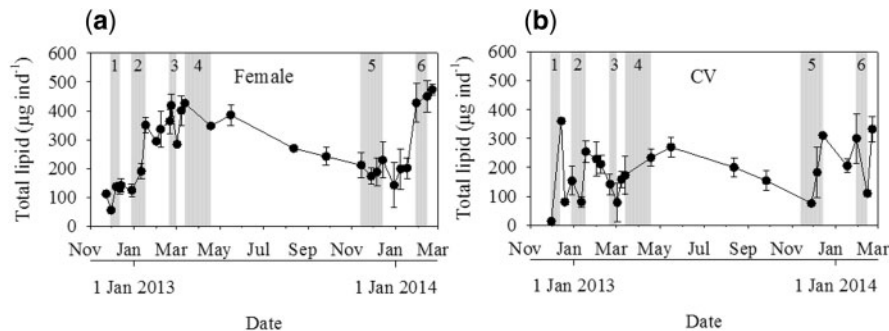
VME 3 (second diapause termination in S1), female TL peaked at 419 $\mu\text{g ind}^{-1}$ on 22 February and declined to 284 $\mu\text{g ind}^{-1}$ at the end (2 March, Figure 6a), and female WE unsaturation declined from 66 to 32% (20 February–3 March, Figure 7a). This suggests lipid utilization by females during VME 3. Although abundances were low, the highest TL content of females during S1 occurred at the start of VME 4 (13 March, 426 $\mu\text{g ind}^{-1}$, Figure 6a); however, unsaturation continued to increase until the end (57% on 18

April, Figure 7a) at the same time as peak unsaturation of CV WE (71%, Figure 7b).

Similar to females, CV TL content (Figure 6b) and WE unsaturation (Figure 7b) were low (12 $\mu\text{g ind}^{-1}$ and 11%, respectively) at the beginning of S1 (similar to abundances) and increased to 254 $\mu\text{g ind}^{-1}$ on 17 January (Figure 6b) and 61% on 11 January (Figure 7b). A decline in CV TL followed between 17 January and 2 March (down to 78 $\mu\text{g ind}^{-1}$) and coincided with the

Table 3. Temporal dynamics of adult male *C. acutus* FAs (FA %) per copepod

Month year	CVI male FA %: mean (n = 6)																						
	December 2012		January 2013		February 2013		March 2013		April 2013		May 2013		August 2013		September 2013		November 2013		December 2013		January 2014		February 2014
Day/FA	19	29	17	20	8	13	18	16	12	26	14	28	6	14	30	17	30	14	21				
10:0	-	-	-	-	-	-	-	-	-	-	-	-	12.9	2.5	7.2	-	-	-	-	-	-	-	-
14:0	-	-	-	-	-	-	-	-	-	-	-	-	6.4	4.5	5.1	-	-	-	-	-	-	-	-
15:0	-	-	-	-	-	-	-	-	-	-	-	-	0.0	0.0	0.0	-	-	-	-	-	-	-	-
16:0	-	-	-	-	-	-	-	-	-	-	-	-	7.7	10.7	6.8	-	-	-	-	-	-	-	-
16:1(n-7)	-	-	-	-	-	-	-	-	-	-	-	-	7.3	3.0	3.5	-	-	-	-	-	-	-	-
16:4(n-1)	-	-	-	-	-	-	-	-	-	-	-	-	0.0	0.0	0.0	-	-	-	-	-	-	-	-
17:0	-	-	-	-	-	-	-	-	-	-	-	-	0.0	0.0	0.0	-	-	-	-	-	-	-	-
18:1(n-9)	-	-	-	-	-	-	-	-	-	-	-	-	2.3	3.3	3.6	-	-	-	-	-	-	-	-
18:1(n-7)	-	-	-	-	-	-	-	-	-	-	-	-	0.0	0.0	0.0	-	-	-	-	-	-	-	-
18:4(n-3)	-	-	-	-	-	-	-	-	-	-	-	-	0.0	0.0	0.0	-	-	-	-	-	-	-	-
20:1(n-9)	-	-	-	-	-	-	-	-	-	-	-	-	13.0	22.0	31.4	-	-	-	-	-	-	-	-
20:3(n-3)	-	-	-	-	-	-	-	-	-	-	-	-	8.6	0.0	0.0	-	-	-	-	-	-	-	-
20:4(n-3)	-	-	-	-	-	-	-	-	-	-	-	-	0.0	0.0	0.0	-	-	-	-	-	-	-	-
22:1(n-11)	-	-	-	-	-	-	-	-	-	-	-	-	8.3	11.8	13.0	-	-	-	-	-	-	-	-
20:5(n-3)	-	-	-	-	-	-	-	-	-	-	-	-	12.0	17.8	14.5	-	-	-	-	-	-	-	-
22:6(n-3)	-	-	-	-	-	-	-	-	-	-	-	-	21.4	24.3	14.9	-	-	-	-	-	-	-	-
Saturated	-	-	-	-	-	-	-	-	-	-	-	-	27.1	17.8	19.1	-	-	-	-	-	-	-	-
Monounsaturated	-	-	-	-	-	-	-	-	-	-	-	-	30.9	40.1	51.5	-	-	-	-	-	-	-	-
Polyunsaturated	-	-	-	-	-	-	-	-	-	-	-	-	42.0	42.1	29.4	-	-	-	-	-	-	-	-

**Figure 6.** Time series of TL content per copepod ($\mu\text{g ind}^{-1}$) for (a) female *C. acutus* and (b) CV *C. acutus*. Shaded areas (grey) represent time periods of VMEs 1–6. Error bars represent ± 1 standard error.

appearance of greater numbers of CIII and CIV stages; however, WE unsaturation remained relatively high ($>51\%$) during this time (Figure 7b). WE unsaturation of both CVs and females peaked on 18 April (71 and 57%, respectively, Figure 7b) at the end of VME 4; however, the TL content of CVs continued to increase until 16 May (to $270 \mu\text{g ind}^{-1}$, Figure 6b), at the same time as a quantitatively similar rise in female TL (Figure 6a). Prior to overwintering, female unsaturation increased to 57% on 18 April and declined to 32% on 14 November, a 25% decrease during dormancy (Figure 7a). Although female TL (in S1) peaked on 13 March at the start of VME 4 ($426 \mu\text{g ind}^{-1}$, Figure 6a), TL was lower at the end of VME 4 on 18 April ($347 \mu\text{g ind}^{-1}$), increased to $385 \mu\text{g ind}^{-1}$ on 16 May, and declined to $212 \mu\text{g ind}^{-1}$ on 14 November (start of VME 5). This corresponds to a decrease of $174 \mu\text{g TL ind}^{-1}$ (16 May to 14 November) and $130 \mu\text{g ind}^{-1}$ of PUWE. CVs were absent in net hauls on 14 November; therefore, winter CV lipid utilization estimates cannot be calculated.

At the end of the main overwintering period, male numbers were still relatively high ($9 \text{ ind } 100 \text{ m}^{-3}$ on 14 November,

Figure 3e); however, their TL content ($27 \mu\text{g ind}^{-1}$, Supplementary Online Resource 2e) and WE unsaturation (12%, Supplementary Online Resource 3e) were low and remained low (TL $20\text{--}30 \mu\text{g ind}^{-1}$, unsaturation 21–25%) until male abundance declined to zero after 7 December (Figure 3e). Females dominated the population at the beginning of S2 and, similar to S1, TL remained relatively constant during dormancy termination (VME 5, $173\text{--}229 \mu\text{g ind}^{-1}$, Figure 6a), unlike WE unsaturation that declined from 32 to 21% (Figure 7a). The TL content of females at the start of S2 (VME 5) was higher than at the start of S1 (VME 1, $137\text{--}132 \mu\text{g ind}^{-1}$); however, declines in WE unsaturation were highly similar between seasons (from 31 to 22% in VME 1). At the start of VME 6 (female dormancy initiation in S2), the TL content of females had rapidly increased to $427 \mu\text{g ind}^{-1}$ with 64% unsaturation (Figures 6a and 7a, respectively). Although female WE unsaturation of 49% at VME 2 (Figure 7a) suggests this level was sufficient for dormancy, the second high biomass diatom bloom of S1 (Figure 2) allowed females to increase their TL content and unsaturation at the end of the productive season

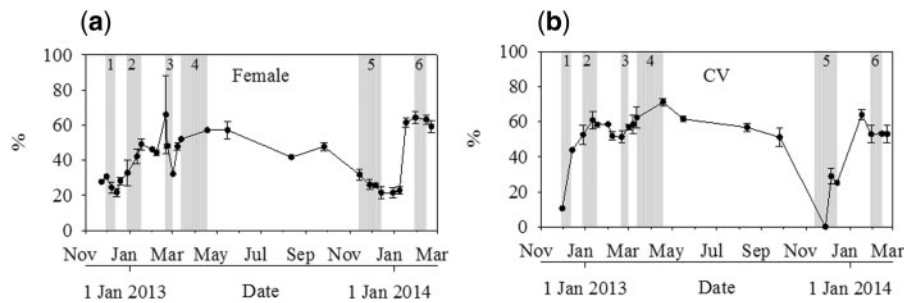


Figure 7. Time series documenting changes in WE unsaturation (%) in (a) females and (b) CVs. Shaded areas (grey) represent time periods of VMEs 1–6. Error bars represent ± 1 standard error.

(VME 4, $426 \mu\text{g ind}^{-1}$ and 57%, respectively), similar to those of females in S2 (at VME 6, Figures 6 and 7).

Discussion

Chl *a* and VMEs

Although patchiness in time and space may theoretically have influenced the results, duplicate net hauls were comparable (slope of linear regression = 0.92, $r^2 = 0.84$, $p < 0.0001$, [Supplementary Online Resource 4](#)) and deep mixed layer depths (MLD) due to storm events were rare (maximum MLD of 112 m during winter 2013, data not shown) indicating that mixing events did not affect the vertical distribution of individuals ([Clarke et al., 2008](#); [Dong et al., 2008](#)).

In this study, the timing of ontogenetic VMEs suggests that dormancy was initiated by females as soon as sufficient stores of TL and PUWE were accumulated. This could have consequences for predators of copepods in surface waters as lipid-rich females were only available for ~ 2 weeks during the first half of January in S1 and 2–4 weeks in S2 (from mid-January to mid-February), after which females migrated to below the base of the thermocline (~ 200 m) and a portion of carbon stored as lipids was sequestered to the deep ocean as a consequence of respiration during dormancy ([Jónasdóttir et al., 2015](#)).

VMEs were linked to the seasonal dynamics of Chl *a*, i.e. the frequency and duration of phytoplankton blooms. Dormancy termination was timed to coincide with high biomass blooms that consisted both of micro-sized (VME 1) and nano-sized (VME 3 and 5) diatoms ([Biggs et al., 2019](#)). *Calanoides acutus* is primarily herbivorous with a short reproductive period that was timed to coincide with high phytoplankton food availability ([Atkinson, 1998](#); [Pasternak and Schnack-Schiel, 2001a](#)). Furthermore, the second ascent of females in S1 (VME 3) indicated that the high biomass diatom bloom provided a strong cue for ascent ([Dezutter et al., 2019](#)), even though female levels of TL ($364\text{--}419 \mu\text{g l}^{-1}$) and unsaturation (66–48%) were still high, and only 34–64 days (VME 2–3) after the initial descent (VME 2). VME 3 represented the mass movement of carbon from deep to shallow water and may have allowed surface-dwelling predators access to an additional peak in the abundance of lipid-rich copepods. Prior to dormancy initiation (VME 2, 4 and 6), it is likely that individuals can directly sense reducing/low phytoplankton food concentrations ([Bautista and Harris, 1992](#); [Perissinotto, 1992](#); [Atkinson, 1994](#); [Pasternak and Schnack-Schiel, 2001a](#); [Garrido et al., 2013](#)); however, at dormancy depths (500–200 m), signals of phytoplankton biomass (at the surface) must be transmitted through the water column and are likely related to sedimentation of

organic matter ([Annett et al., 2010](#); [Ducklow et al., 2012](#); [Turner, 2015](#)). During winter, when Chl *a* concentrations are low, increased proportions of smaller flagellated phytoplankton are observed ([Rozema et al., 2017](#)) and the shift to a high biomass, diatom-dominated period (at VME 1 and 5) most likely promoted a more herbivorous diet with reduced coprophagy/coprorhexy ([Pasternak and Schnack-Schiel, 2001a, b](#); [Turner, 2002, 2015](#)) and (at the same time as increased stratification during VME 1 and 5; [Biggs et al., 2019](#)) increased the load and sinking speed of faecal pellets (FPs) in the water column. Similarly, a relatively low biomass, flagellate-dominated period ([Biggs et al., 2019](#)) was observed prior to the second high biomass diatom bloom in S1, and the second ascent of females (VME 3). FPs produced from flagellated phytoplankton diets have been observed to sink almost ten times slower than diatom fed pellets ([Ploug et al., 2008](#)), likely related to mineral ballasting by biogenic silica ([Voss, 1991](#)). Diatoms also produce transparent exopolymer particles (TEPs) in abundance and are a major component of diatom aggregates ([Passow, 2002](#)). TEPs production combined with organic material released from melting sea ice (and increased stratification) may produce further deposition resulting in a rain of organic material at depth. Rapidly sinking FPs ($>300 \text{ m d}^{-1}$) ([Ploug et al., 2008](#); [Atkinson et al., 2012a](#)) would enable organic material to reach the overwintering population of *C. acutus* (500–200 m) within 1–2 days and pigment degradation products, characteristic of the phytoplankton community, can be detected in FPs ([Nelson, 1989](#)). Microbial degradation of sedimenting organic matter may leak solutes into the surrounding water ([Turner, 2015](#)), which, through chemosensory mechanisms and probably hormonally mediated, may trigger the ascent ([Irigoin, 2004](#)).

Losses

Declines in abundance over the winter period (a 68% reduction between April and November 2013, VME 4–5, [Supplementary Online Resource 5](#)) suggest the $64 \text{ ind } 100 \text{ m}^{-3}$ at the start of S1 (total population abundance at VME 1) each needed to contribute ~ 3 offspring (total of $192 \text{ ind } 100 \text{ m}^{-3}$ required on 18 April 2013) to balance losses during winter. At dormancy initiation (VME 4), population numbers were 48% less ($100 \text{ ind } 100 \text{ m}^{-3}$ captured on 18 April 2013) representing (in retrospect) a minimum total requirement of $\sim 6 \text{ ind female}^{-1}$, over S1 and winter combined, to maintain the population over an annual cycle. This indicates during S1 either loss rates were twice as high (to maintain the population) or egg production twice as low. Low egg production may be related to relatively lower TL stores at the start of

S1, compared with S2 (VME 1, $137 \pm 5 \mu\text{g ind}^{-1}$, $n=3$; VME 5, $200 \pm 25 \mu\text{g ind}^{-1}$, $n=4$) as well as reduced CI–CIV recruitment ($1266 \text{ ind } 100 \text{ m}^{-3}$ at initial CI peaks in S1 and $3106 \text{ ind } 100 \text{ m}^{-3}$ in S2). Whilst the large amounts of lipid and high unsaturation alone could have triggered entrance into dormancy at VME 2 and 6, lower TL and unsaturation were observed at VME 2 compared with VME 6 (Figures 6 and 7). Eggs, nauplii, copepodites, and potentially even adults of *C. acutus* are within the potential prey range for many of the large zooplankton species that were often observed during both seasons, such as *Metridia gerlachei*, *Rhincalanus gigas*, (*Para*)*euchaeta antarctica*, euphausiids, polychaetes and arrow worms. The 1 month earlier increase in larger-sized zooplankton abundance ($>200 \mu\text{m}$) in S1 than in S2 (Supplementary Online Resource 6) matched the 1 month earlier descent of female *C. acutus*, which may imply that enhanced predation pressure affects the initial decision of females to descend. The combination of increased numbers of larger-sized zooplankton and reducing/low Chl *a* concentrations (January S1) may have resulted in even higher predation pressure on smaller zooplankton (including nauplii and copepodites) by larger omnivorous individuals (Pasternak and Schnack-Schiel, 2001a) and contribute to high losses over S1.

The nano-sized cells during the second high biomass diatom bloom in S1 (Biggs et al., 2019) likely represented a suitable prey size for copepodites (Perissinotto, 1992) as they mature and attempt to increase lipid stores at the end of the productive season; however, relatively low TL content of CVs was observed ($270 \mu\text{g ind}^{-1}$) at diapause initiation (VME 4). The biomass dominant phytoplankton population during this bloom ($11 \mu\text{m}$ \varnothing diatom) was subjected to high rates of viral lysis (Biggs et al., unpublished), which may have reduced food availability during a crucial time of lipid accumulation prior to diapause. Increased substrate availability (due to the viral shunt) could explain the S1 peak in bacteria abundance mid-March (Biggs et al., unpublished), which likely benefitted micro-zooplankton grazers (Azam et al., 1991). Although considered primarily herbivorous, low phytoplankton abundance could stimulate carnivorous grazing (Pasternak and Schnack-Schiel, 2001a) by late-season recruits and explain why CV TL increased between 18 April and 16 May (from 233 to $270 \mu\text{g ind}^{-1}$) whilst WE unsaturation declined (from 71 to 61%). Reduced lipid stores combined with a relatively shallow diapause depth ($<500 \text{ m}$) could be related to high winter mortality as deeper depths may allow females to better take advantage of the lipid phase transition effects of a highly unsaturated ($\sim 50\%$) lipid store (Pond and Tarling, 2011). If neutral buoyancy cannot be achieved, then high rates of lipid utilization and mortality may be due to additional energetic costs associated with swimming to maintain an optimum position in the water column. At the same time, predation pressures may be higher in the top 500 m than below (Yamaguchi et al., 2004; Harper and Peck, 2016) and individuals close to the bottom depth, where phase transition of WEs may occur, would be more concentrated and exposed to the benthic community. The relatively high unsaturation of CVs (compared with females) at the time of overwintering (71–61%) and low TL (233 – $270 \mu\text{g ind}^{-1}$ representing 132 – $140 \mu\text{g ind}^{-1}$ of PUWE and ~ 32 – $34 \mu\text{g ind}^{-1}$ EPA) suggests that increased unsaturation was prioritized when TL was increased. The data of Pond and Tarling (2011) also indicate that, at depths $<500 \text{ m}$, WE phase transition occurred at higher temperatures and was more pronounced at higher levels of unsaturation (70%). The greater increase in the unsaturation of CV WE prior to diapause

may have been a mechanism to compensate for lower TL stores and take advantage of energetic savings at higher temperatures as lipid stores become increasingly dense with depth.

Diapause mechanisms and life cycle

The level of unsaturation of the WE lipid store, rather than the total amount (TL), is potentially a key mechanism influencing the dormancy behaviour of calanoid copepods (Pond and Tarling, 2011; Pond et al., 2012). In our study, unsaturation levels peaked at the start of the main dormancy period (VME 4) and declined over the winter. Dynamics were determined by the retention of FA 20:1(n-9) and 22:1(n-11) (during winter) and the selective accumulation (during summer) and utilization (during winter) of 20:5(n-3) (EPA). Changes in unsaturation were often not mirrored by changes in TL indicating a more functional role of FA composition. EPA is a precursor of eicosanoids that are locally acting “tissue hormones” and may influence functions such as reproduction, ion, and water transport (Persson and Vrede, 2006). The WE of many herbivorous copepods is also characterized by considerable amounts of long-chain monounsaturated fatty alcohols [20:1(n-9) and 22:1(n-11)], which are not present in significant amounts in their phytoplankton diet (Albers et al., 1996; Lee et al., 2006; Pond et al., 2012). This biosynthesis of fatty alcohols and esterification with FA to WE resulted in rapid lipid accumulation since there is both *de novo* synthesis and incorporation of dietary lipids (Graeve et al., 2005). During increases in unsaturation (summer), stores of 20:1(n-9) and 22:1(n-11) (retained during winter) are likely reduced to fatty alcohols (Kattner et al., 1994; Pond et al., 2012) and esterified to 20:5(n-3) acquired from dietary sources. Unsaturation level of the entire lipid store was therefore determined by synergistic changes in “pools” of 20:1(n-9) + 22:1(n-11) and 20:5(n-3), rather than unsaturation dynamics determined solely by 20:5(n-3). This action has a double impact on unsaturation levels (+1 PUFA, –1 MUFA), as FAs are converted to fatty alcohols (and vice versa), likely providing a stable signal regarding changes in unsaturation state. The physiological impact of selective EPA utilization during dormancy may further act as a biological timer (Häfker et al., 2017, 2018) and, combined with increased buoyancy (due to reducing unsaturation and phase transition), could stimulate ascent. In relatively deep waters of the Scotia sea, late-stage *C. acutus* individuals that typically diapause between 500 and 1000 m or deeper were observed with a tri-modal vertical distribution at one site (<100 , 400–600, and 800–1000 m) and concentrated in the 300–500 m depth range at another (Pond et al., 2012). One explanation for this is that individuals had ascended from deeper waters to an intermediate depth to await the initiation of the “Spring” bloom (Pond et al., 2012). This initial “intermediate” migration is potentially triggered by reduced levels of unsaturation; however, in coastal and relatively shallow shelf sea areas such as Ryder Bay, bottom depth (520 m) is similar to this intermediate depth; therefore, signals of reduced unsaturation and increased phytoplankton standing stock may combine to initiate ascent.

The late-season high biomass diatom bloom of S1 coincided with the second ascent of females (VME 3) at the same time as lipids appear to be utilized (TL decreased from 419 to $284 \mu\text{g ind}^{-1}$ and WE unsaturation decreased from 66 to 32%). The second S1 spawning event coincided with a decline in total female abundance over VME 3 (from 31 to 9 ind 100 m^{-3} ,

Supplementary Online Resource 5a) and suggests that the ascending females that spawned expired after a 1-year life cycle. In contrast during S2, a singular but prolonged high biomass bloom (Figure 2) resulted in a singular spawning event and a 1-month delay in dormancy initiation of (most likely “new”) females. Chl *a* concentrations were relatively low between 21 February and 15 April post-S2 ($1.5 \pm 0.7 \mu\text{g l}^{-1}$, $n=8$), and these females likely remained in dormancy to complete a 2-year life cycle. Such a mechanism could explain why some studies suggest the overwintering stages of *C. acutus* complete their life cycle in 1 year (Marin, 1988; Quetin *et al.*, 1996; Atkinson *et al.*, 1997) and others that they re-enter diapause and survive an extra year (Hagen and Schnack-Schiel, 1996; Tarling *et al.*, 2004). The late-season phytoplankton bloom in S1 was associated with higher temperature (Biggs *et al.*, 2019), similar to novel autumn blooms observed in the Arctic (Ardyna *et al.*, 2014), and suggests that global warming could influence the lifespan of vertically migrating copepods and promote a 1-year life cycle, rather than a 2-year life cycle.

Although two spawning events were observed in S1, the abundance of CI–IV in shallow water on 2 March 2013 (initial peak of 531 ind 100 m^{-3}) was similar to 17 January 2013 (735 ind 100 m^{-3}). Maturing copepodites from the late-season spawning event would likely benefit from reduced predation pressure due to lower numbers of larger-sized zooplankton and an abundance of phytoplankton food (Pasternak and Schnack-Schiel, 2001a) and could explain the similarity in CI–CIV numbers, even though peak shallow female abundance was threefold higher during VME 1 (108 ind 100 m^{-3}) than VME 3 (33 ind 100 m^{-3}). Conversely, copepodites from the early-season spawning event would have matured during times of low Chl *a* (food availability) with increased proportions of cryptophytes (preference of diatoms as food type; Verity and Smayda, 1989; Head and Harris, 1994) and high numbers of larger-sized zooplankton (high predation pressure, Pasternak and Schnack-Schiel, 2001a). An early-season mismatch and late-season match, between peaks of Chl *a*, new *C. acutus* recruits and higher trophic predators (Durant *et al.*, 2013), likely resulted in a relatively greater contribution of individuals from the late-season spawning event to annual reproductive success. This flexible dormancy strategy would enable females to maximize phytoplankton food availability and reproductive capability whilst reducing predation risk.

It is likely that multiple internal and external factors combine, such as a lipid-modulated endogenous clock (Johnson *et al.*, 2008; Häfker *et al.*, 2018), TL content (to support reproductive maturation and winter survival; Hagen and Schnack-Schiel, 1996; Rey-Rassat *et al.*, 2002), WE unsaturation (buoyancy regulation; Pond *et al.*, 2012), and food availability (Friedland *et al.*, 2016) to serve as a timing mechanism to determine ontogenetic vertical migration behaviour.

Conclusions

The dormancy behaviour of *C. acutus* CV and CVI stages appears coupled to the frequency and duration of phytoplankton blooms. Dormancy termination post-winter coincided with reduced unsaturation (~30%) and increased phytoplankton standing stock. Once sufficient lipid stores were accumulated after the initial phytoplankton bloom period (350 $\mu\text{g TL ind}^{-1}$ with ~49% unsaturation), dormancy was initiated when Chl *a* concentrations declined. An early S1 increase in larger-sized zooplankton numbers (compared with S2) likely contributed to increased losses

and early dormancy initiation. A late summer diatom bloom, driven by higher temperatures, stimulated ascent and spawning of dormant females for the second time in S1 and the resulting late-season copepodites would benefit from reduced predation (low numbers of larger-sized zooplankton) and high phytoplankton food availability, i.e. a match between peaks of Chl *a*, new *C. acutus* recruits, and higher trophic predators. The loss of females during dormancy termination (VME 3) suggests that individuals expire after two main “spawning events”. Furthermore, the timing of these events is regulated by the frequency and duration of phytoplankton blooms, which have consequences for the lifespan of *C. acutus* females, either 1 or 2 years. This flexible strategy would enable females to maximize phytoplankton food availability and reduce the likelihood of predation, thereby increasing reproductive capability whilst promoting the survival of produced offspring via reduced mortality rates. As such, dormancy behaviour and copepod lifespan, and thus zooplankton’s role in the biological carbon pump, are intimately linked to the structure and dynamics of the Southern Ocean food web.

Supplementary data

Supplementary material is available at the ICESJMS online version of the manuscript.

Acknowledgements

We wish to thank the British Antarctic Survey for their logistical support and cooperation during the field campaign. This work was part of the ANTPHIRCO project (grant 866.10.102 awarded to CPDB), which was supported by the Earth and Life Sciences Foundation (ALW), with financial aid from the Netherlands Organisation for Scientific Research (NWO). We are also extremely grateful to Prof Stefan Schouten at the Royal Netherlands Institute for Sea Research (NIOZ) for his expertise and support. Furthermore, we wish to thank Dr Amber Annett, Zoi Farenzena, and Dorien Verheyen for their help and support during the field campaign as well as Santiago Gonzalez and Anna Noordeloos for their technical support at the NIOZ.

References

- Albers, C. S., Kattner, G., and Hagen, W. 1996. The compositions of wax esters, triacylglycerols and phospholipids in Arctic and Antarctic copepods: evidence of energetic adaptations. *Marine Chemistry*, 55: 347–358.
- Annett, A. L., Carson, D. S., Crosta, X., Clarke, A., and Ganeshram, R. S. 2010. Seasonal progression of diatom assemblages in surface waters of Ryder Bay, Antarctica. *Polar Biology*, 33: 13–29.
- Ardyna, M., Babin, M., Gosselin, M., Devred, E., Rainville, L., and Tremblay, J.-É. 2014. Recent Arctic Ocean sea ice loss triggers novel fall phytoplankton blooms. *Geophysical Research Letters*, 41: 6207–6212.
- Atkinson, A. 1994. Diets and feeding selectivity among theepipelagic copepod community near South Georgia in summer. *Polar Biology*, 14: 551–560.
- Atkinson, A. 1998. Life cycle strategies of epipelagic copepods in the Southern Ocean. *Journal of Marine Systems*, 15: 289–311.
- Atkinson, A., Schmidt, K., Fielding, S., Kawaguchi, S., and Geissler, P. A. 2012a. Variable food absorption by Antarctic krill: relationships between diet, egestion rate and the composition and sinking rates of their fecal pellets. *Deep-Sea Research Part II: Topical Studies in Oceanography*, 59–60: 147–158.
- Atkinson, A., Schnack-Schiel, S., Ward, P., and Marin, V. 1997. Regional differences in the life cycle of *Calanoides acutus*

- (Copepoda: Calanoida) within the Atlantic sector of the Southern Ocean. *Marine Ecology Progress Series*, 150: 99–111.
- Atkinson, A., Ward, P., Hunt, B. P. V., Pakhomov, E. A., and Hsieh, G. W. 2012b. An overview of Southern Ocean zooplankton data: abundance, biomass, feeding and functional relationships. *CCAMLR Science*, 19: 171–218.
- Azam, F., Smith, D. C., and Hollibaugh, J. T. 1991. The role of the microbial loop in Antarctic pelagic ecosystems. *Polar Research*, 10: 239–244.
- Baumgartner, M. F., and Tarrant, A. M. 2017. The physiology and ecology of diapause in marine copepods. *Annual Review of Marine Science*, 9: 387–411.
- Bautista, B., and Harris, R. P. 1992. Copepod gut contents, ingestion rates and grazing impact on phytoplankton in relation to size structure of zooplankton and phytoplankton during a spring bloom. *Marine Ecology Progress Series*, 82: 41–50.
- Beardsley, R. C., Limeburner, R., and Brechner Owens, W. 2004. Drifter measurements of surface currents near Marguerite Bay on the western Antarctic Peninsula shelf during austral summer and fall, 2001 and 2002. *Deep-Sea Research Part II: Topical Studies in Oceanography*, 51: 1947–1964.
- Biggs, T. E. G., Alvarez-Fernandez, S., Evans, C., Mojica, K. D. A., Rozema, P. D., Venables, H. J., Pond, D. W., et al. 2019. Antarctic phytoplankton community composition and size structure: importance of ice type and temperature as regulatory factors. *Polar Biology*, 42: 1997–2015.
- Budge, S. M., Iverson, S. J., and Koopman, H. N. 2006. Studying trophic ecology in marine ecosystems using fatty acids: a primer on analysis and interpretation. *Marine Mammal Science*, 22: 759–801.
- Clark, K. A. J., Brierley, A. S., and Pond, D. W. 2012. Composition of wax esters is linked to diapause behavior of *Calanus finmarchicus* in a sea loch environment. *Limnology and Oceanography*, 57: 65–75.
- Clarke, A., Meredith, M. P., Wallace, M. I., Brandon, M. A., and Thomas, D. N. 2008. Seasonal and interannual variability in temperature, chlorophyll and macronutrients in northern Marguerite Bay, Antarctica. *Deep-Sea Research Part II: Topical Studies in Oceanography*, 55: 1988–2006.
- Dezutter, T., Lalande, C., Dufresne, C., Darnis, G., and Fortier, L. 2019. Mismatch between microalgae and herbivorous copepods due to the record sea ice minimum extent of 2012 and the late sea ice break-up of 2013 in the Beaufort Sea. *Progress in Oceanography*, 173: 66–77.
- Dong, S., Sprintall, J., Gille, S. T., and Talley, L. 2008. Southern Ocean mixed-layer depth from Argo float profiles. *Journal of Geophysical Research*, 113: C06013.
- Drits, A. V., Pasternak, A. F., and Kosobokova, K. N. 1994. Physiological characteristics of the antarctic copepod *Calanoides acutus* during late summer in the Weddell Sea. *Hydrobiologia*, 292–293: 201–207.
- Drits, A. V., Pasternak, A. F., and Kosobokova, K. N. 1994. Physiological characteristics of the Antarctic copepod *Calanoides acutus* during late summer in the Weddell Sea. *Hydrobiologia*, 292–293: 201–207.
- Ducklow, H., Clarke, A., Dickhut, R., Doney, S. C., Geisz, H., Huang, K., Martinson, D. G., et al. 2012. The marine system of the Western Antarctic Peninsula. *Antarctic Ecosystems*, 5: 121–159.
- Durant, J., Hjermann, D., Falkenhaus, T., Gifford, D., Naustvoll, L., Sullivan, B., Beaugrand, G., et al. 2013. Extension of the match-mismatch hypothesis to predator-controlled systems. *Marine Ecology Progress Series*, 474: 43–52.
- Falk-Petersen, S., Hagen, W., Kattner, G., Clarke, A., and Sargent, J. 2000. Lipids, trophic relationships, and biodiversity in Arctic and Antarctic krill. *Canadian Journal of Fisheries and Aquatic Sciences*, 57: 178–191.
- Falk-Petersen, S., Mayzaud, P., Kattner, G., and Sargent, J. R. 2009. Lipids and life strategy of Arctic *Calanus*. *Marine Biology Research*, 5: 18–39.
- Friedland, K. D., Record, N. R., Asch, R. G., Kristiansen, T., Saba, V. S., Drinkwater, K. F., Henson, S., et al. 2016. Seasonal phytoplankton blooms in the North Atlantic linked to the overwintering strategies of copepods. *Elementa: Science of the Anthropocene*, 4: 000099.
- Garrido, S., Cruz, J., Santos, A. M. P., Ré, P., and Saiz, E. 2013. Effects of temperature, food type and food concentration on the grazing of the calanoid copepod *Centropages chierchiae*. *Journal of Plankton Research*, 35: 843–854.
- Graeve, M., Albers, C., and Kattner, G. 2005. Assimilation and biosynthesis of lipids in Arctic *Calanus* species based on feeding experiments with a ¹³C labelled diatom. *Journal of Experimental Marine Biology and Ecology*, 317: 109–125.
- Graeve, M., Kattner, G., and Hagen, W. 1994. Diet-induced changes in the fatty acid composition of Arctic herbivorous copepods: experimental evidence of trophic markers. *Journal of Experimental Marine Biology and Ecology*, 182: 97–110.
- Häfker, N. S., Meyer, B., Last, K. S., Pond, D. W., Hüppe, L., and Teschke, M. 2017. Circadian clock involvement in zooplankton diel vertical migration. *Current Biology*, 27: 2194–2201.e3.
- Häfker, N. S., Teschke, M., Last, K. S., Pond, D. W., Hüppe, L., and Meyer, B. 2018. *Calanus finmarchicus* seasonal cycle and diapause in relation to gene expression, physiology, and endogenous clocks. *Limnology and Oceanography*, 63: 2815–2838.
- Hagen, W., Kattner, G., and Graeve, M. 1993. *Calanoides acutus* and *Calanus propinquus*, Antarctic copepods with different lipid storage modes via wax esters or triacylglycerols. *Marine Ecology Progress Series*, 97: 135–142.
- Hagen, W., and Schnack-Schiel, S. B. 1996. Seasonal lipid dynamics in dominant Antarctic copepods: energy for overwintering or reproduction? *Deep-Sea Research Part I: Oceanographic Research Papers*, 43: 139–158.
- Harper, E. M., and Peck, L. S. 2016. Latitudinal and depth gradients in marine predation pressure. *Global Ecology and Biogeography*, 25: 670–678.
- Head, E. J. H., and Harris, L. R. 1994. Feeding selectivity by copepods grazing on natural mixtures of phytoplankton determined by HPLC analysis of pigments. *Marine Ecology Progress Series*, 110: 75–84.
- Heath, M. R., Boyle, P. R., Gislason, A., Gurney, W. S. C., Hay, S. J., Head, E. J. H., Holmes, S., et al. 2004. Comparative ecology of over-wintering *Calanus finmarchicus* in the northern North Atlantic, and implications for life-cycle patterns. *ICES Journal of Marine Science*, 61: 698–708.
- Hopkins, T. L., and Torres, J. J. 1989. Midwater food web in the vicinity of a marginal ice zone in the western Weddell Sea. *Deep Sea Research Part A. Oceanographic Research Papers*, 36: 543–560.
- Huisman, J., van Oostveen, P., and Weissing, F. J. 1999. Critical depth and critical turbulence: two different mechanisms for the development of phytoplankton blooms. *Limnology and Oceanography*, 44: 1781–1787.
- Huntley, M., and Escritor, F. 1991. Dynamics of *Calanoides acutus* (Copepoda: Calanoida) in Antarctic coastal waters. *Deep Sea Research Part A, Oceanographic Research Papers*, 38: 1145–1167.
- Irigoin, X. 2004. Some ideas about the role of lipids in the life cycle of *Calanus finmarchicus*. *Journal of Plankton Research*, 26: 259–263.
- Johnson, C. L., Leising, A. W., Runge, J. A., Head, E. J. H., Pepin, P., Plourde, S., and Durbin, E. G. 2008. Characteristics of *Calanus finmarchicus* dormancy patterns in the Northwest Atlantic. *ICES Journal of Marine Science*, 65: 339–350.

- Jónasdóttir, S. H., Visser, A. W., Richardson, K., and Heath, M. R. 2015. Seasonal copepod lipid pump promotes carbon sequestration in the deep North Atlantic. *Proceedings of the National Academy of Sciences of the United States of America*, 112: 12122–12126.
- Kattner, G., Graeve, M., and Hagen, W. 1994. Ontogenetic and seasonal changes in lipid and fatty acid/alcohol compositions of the dominant Antarctic copepods *Calanus propinquus*, *Calanoides acutus* and *Rhincalanus gigas*. *Marine Biology*, 118: 637–644.
- Kattner, G., and Hagen, W. 2009. Lipids in marine copepods: latitudinal characteristics and perspective to global warming. *In* *Lipids in Aquatic Ecosystems*, pp. 257–280. Springer New York, New York, NY.
- Lee, R. F., Hagen, W., and Kattner, G. 2006. Lipid storage in marine zooplankton. *Marine Ecology Progress Series*, 307: 273–306.
- Ma, S., Tao, Z., Yang, X., Yu, Y., Zhou, X., Ma, W., and Li, Z. 2014. Estimation of marine primary productivity from satellite-derived phytoplankton absorption data. *IEEE Journal of Selected Topics in Applied Earth Observations and Remote Sensing*, 7: 3084–3092.
- Maps, F., Record, N. R., and Pershing, A. J. 2014. A metabolic approach to dormancy in pelagic copepods helps explaining inter- and intra-specific variability in life-history strategies. *Journal of Plankton Research*, 36: 18–30.
- Maps, F., Runge, J. A., Leising, A., Pershing, A. J., Record, N. R., Plourde, S., and Pierson, J. J. 2012. Modelling the timing and duration of dormancy in populations of *Calanus finmarchicus* from the Northwest Atlantic shelf. *Journal of Plankton Research*, 34: 36–54.
- Marin, V. 1988. Qualitative models of the life cycles of *Calanoides acutus*, *Calanus propinquus*, and *Rhincalanus gigas*. *Polar Biology*, 8: 439–446.
- Marrari, M., Daly, K. L., Timonin, A., and Semenova, T. 2011. The zooplankton of Marguerite Bay, Western Antarctic Peninsula-Part I: abundance, distribution, and population response to variability in environmental conditions. *Deep-Sea Research Part II: Topical Studies in Oceanography*, 58: 1599–1613.
- Moffat, C., Beardsley, R. C., Owens, B., and van Lipzig, N. 2008. A first description of the Antarctic Peninsula Coastal Current. *Deep Sea Research Part II: Topical Studies in Oceanography*, 55: 277–293.
- Nelson, J. 1989. Phytoplankton pigments in macrozooplankton feces: variability in carotenoid alterations. *Marine Ecology Progress Series*, 52: 129–144.
- Passow, U. 2002. Transparent exopolymer particles (TEP) in aquatic environments. *Progress in Oceanography*, 55: 287–333.
- Pasternak, A. F., and Schnack-Schiel, S. B. 2001a. Seasonal feeding patterns of the dominant Antarctic copepods *Calanus propinquus* and *Calanoides acutus* in the Weddell Sea. *Polar Biology*, 24: 771–784.
- Pasternak, A. F., and Schnack-Schiel, S. B. 2001b. Feeding patterns of dominant Antarctic copepods: an interplay of diapause, selectivity, and availability of food. *Hydrobiologia*, 453–454: 25–36.
- Pepin, P., and Head, E. J. H. 2009. Seasonal and depth-dependent variations in the size and lipid contents of stage 5 copepodites of *Calanus finmarchicus* in the waters of the Newfoundland Shelf and the Labrador Sea. *Deep-Sea Research Part I: Oceanographic Research Papers*, 56: 989–1002.
- Perissinotto, R. 1992. Meso-zooplankton size-selectivity and grazing impact on the phytoplankton community of the Prince Edward Archipelago (Southern Ocean). *Marine Ecology Progress Series*, 79: 243–258.
- Persson, J., and Vrede, T. 2006. Polyunsaturated fatty acids in zooplankton: variation due to taxonomy and trophic position. *Freshwater Biology*, 51: 887–900.
- Pervushin, A. S. 1968. Observations of the behaviour and feeding of whalebone whales in the area of the Crozet Islands. *Oceanology*, 8: 110–115.
- Ploug, H., Iversen, M. H., and Fischer, G. 2008. Ballast, sinking velocity, and apparent diffusivity within marine snow and zooplankton fecal pellets: implications for substrate turnover by attached bacteria. *Limnology and Oceanography*, 53: 1878–1886.
- Pond, D. W., and Tarling, G. A. 2011. Phase transitions of wax esters adjust buoyancy in diapausing *Calanoides acutus*. *Limnology and Oceanography*, 56: 1310–1318.
- Pond, D. W., Tarling, G. A., and Mayor, D. J. 2014. Hydrostatic pressure and temperature effects on the membranes of a seasonally migrating marine copepod. *PLoS One*, 9: e111043.
- Pond, D. W., Tarling, G. A., Ward, P., and Mayor, D. J. 2012. Wax ester composition influences the diapause patterns in the copepod *Calanoides acutus*. *Deep-Sea Research Part II: Topical Studies in Oceanography*, 59–60: 93–104.
- Pond, D. W., Watkins, J., Priddle, J., and Sargent, J. 1995. Variation in the lipid content and composition of Antarctic krill *Euphausia superba* at South Georgia. *Marine Ecology Progress Series*, 117: 49–58.
- Quetin, L. B., Ross, R. M., Frazer, T. K., and Haberman, K. L. 1996. Factors Affecting Distribution and Abundance of Zooplankton, with an Emphasis on Antarctic Krill, *Euphausia superba*. *In* *Foundations for Ecological Research West of the Antarctic Peninsula* (eds R.M. Ross, E.E. Hofmann and L.B. Quetin), pp. 357–371.
- Record, N. R., Ji, R., Maps, F., Varpe, Ø., Runge, J. A., Petrik, C. M., and Johns, D. 2018. Copepod diapause and the biogeography of the marine lipidscape. *Journal of Biogeography*, 45: 2238–2251.
- Rey-Rassat, C., Irigoien, X., Harris, R., and Carlotti, F. 2002. Energetic cost of gonad development in *Calanus finmarchicus* and *C. helgolandicus*. *Marine Ecology Progress Series*, 238: 301–306.
- Rozema, P. D., Venables, H. J., van de Poll, W. H., Clarke, A., Meredith, M. P., and Buma, A. G. J. 2017. Interannual variability in phytoplankton biomass and species composition in northern Marguerite Bay (West Antarctic Peninsula) is governed by both winter sea ice cover and summer stratification. *Limnology and Oceanography*, 62: 235–252.
- Sartoris, F. J., Thomas, D. N., Cornils, A., and Schiela, S. B. S. 2010. Buoyancy and diapause in Antarctic copepods: The role of ammonium accumulation. *Limnology and Oceanography*, 55: 1860–1864.
- Schnack-Schiel, S. B., Hagen, W., and Mizdalski, E. 1991. Seasonal comparison of *Calanoides acutus* and *Calanus propinquus* (Copepoda: Calanoida) in the southeastern Weddell Sea, Antarctica. *Marine Ecology Progress Series*, 70: 17–27.
- Shreeve, R. S., Tarling, G. A., Atkinson, A., Ward, P., Goss, C., and Watkins, J. 2005. Relative production of *Calanoides acutus* (Copepoda: Calanoida) and *Euphausia superba* (Antarctic krill) at South Georgia, and its implications at wider scales. *Marine Ecology Progress Series*, 298: 229–239.
- Smetacek, V., and Nicol, S. 2005. Polar ocean ecosystems in a changing world. *Nature*, 437: 362–368.
- Sommer, U., and Lengfellner, K. 2008. Climate change and the timing, magnitude, and composition of the phytoplankton spring bloom. *Global Change Biology*, 14: 1199–1208.
- Stevens, C. J., Deibel, D., and Parrish, C. C. 2004. Incorporation of bacterial fatty acids and changes in a wax ester-based omnivory index during a long-term incubation experiment with *Calanus glocalis* Jaschnov. *Journal of Experimental Marine Biology and Ecology*, 303: 135–156.
- Sverdrup, H. 1953. On conditions for the vernal blooming of phytoplankton. *ICES Journal of Marine Science*, 18: 287–295.
- Tarling, G. A., Shreeve, R. S., Ward, P., Atkinson, A., and Hirst, A. G. 2004. Life-cycle phenotypic composition and mortality of *Calanoides acutus* (Copepoda: Calanoida) in the Scotia Sea: a

- modelling approach. *Marine Ecology Progress Series*, 272: 165–181.
- Turner, J. 2002. Zooplankton fecal pellets, marine snow and sinking phytoplankton blooms. *Aquatic Microbial Ecology*, 27: 57–102.
- Turner, J. T. 2015. Zooplankton fecal pellets, marine snow, phytodetritus and the ocean's biological pump. *Progress in Oceanography*, 130: 205–248.
- Verity, P. G., and Smayda, T. J. 1989. Nutritional value of *Phaeocystis pouchetii* (Prymnesiophyceae) and other phytoplankton for *Acartia* spp. (Copepoda): Ingestion, egg production, and growth of nauplii. *Marine Biology*, 100: 161–171.
- Visser, A. W., and Jónasdóttir, S. H. 1999. Lipids, buoyancy and the seasonal vertical migration of *Calanus finmarchicus*. *Fisheries Oceanography*, 8: 100–106.
- Voronina, N. 1998. Comparative abundance and distribution of major filter-feeders in the Antarctic pelagic zone. *Journal of Marine Systems*, 17: 375–390.
- Voss, M. 1991. Content of copepod faecal pellets in relation to food supply in Kiel Bight and its effect on sedimentation rate. *Marine Ecology Progress Series*, 75: 217–225.
- Yamaguchi, A., Ikeda, T., Watanabe, Y., and Ishizaka, J. 2004. Vertical distribution patterns of pelagic copepods as viewed from the predation pressure hypothesis. *Zoological Studies*, 43: 475–485.

Handling editor: Rubao Ji